Strong perpendicular magnetic anisotropy of Fe–Pd nanocrystalline particles enhanced by Co addition

András Kovács,[a] Kazuhisa Sato, and Yoshihiko Hirotsu
The Institute of Scientific and Industrial Research, Osaka University, 8-1 Mihogaoka, Ibaraki, Osaka 567-0047, Japan

(Received 21 July 2006; accepted 6 December 2006; published online 12 February 2007)

$L1_0$-PdCoFe nanoparticles were prepared by vapor deposition of the components and characterized by transmission electron microscopy and by superconducting quantum interference device magnetometry. Co addition to the Fe–Pd nanocrystals resulted in a strong perpendicular magnetic anisotropy and a reduction in the formation temperature of the ordered $L1_0$ phase. Formation of the ordered phase was studied by *in situ* annealing of specimens inside the transmission electron microscope. $L1_0$ phase formation started at 698 K, as evidenced by the appearance of 110 superlattice reflections in electron diffraction patterns. Co additions enhanced the magnetic easy axis alignment perpendicular to the film plane. The perpendicular maximum coercivity at room temperature was 1.75 kOe for $L1_0$-PdCoFe nanoparticles with an average size of 8 nm, and the magnetic coercivity decreased by increasing the Co concentration in the $L1_0$ nanoparticles. © *2007 American Institute of Physics*. [DOI: 10.1063/1.2434958]

I. INTRODUCTION

Single-domain nanoparticles have considerable interest from the standpoint of high-density magnetic recording media technology. $L1_0$ ordered structures such as FePt, FePd, and CoPt are promising materials for this application because of their high uniaxial magnetic anisotropy energies.[1] A number of attempts have been made to fabricate a nanosized island structure consisting of individual $L1_0$ particles by different preparation techniques.[2–4] In general, a reduction in the ordering temperature and alignment of the magnetic easy axis (*c* axis of the tetragonal $L1_0$ structure) are requirements for technological applications. Reduction in $L1_0$ ordering temperature was achieved by adding a third element such as Ag or Cu to FePt thin films.[5,6] Although these elements (Ag and Cu) effectively decrease the $L1_0$ ordering temperature, their presence reduces the magnetic/nonmagnetic ratio of elements in the sample, which can lead to compositional-sensitive magnetic properties.[7] Addition of a magnetic element such as Co can be appropriate for such a purpose; however, no information is available in recent literature about the effects of Co additions on the $L1_0$ ordered phase formation in Fe–Pd system.

In order to utilize $L1_0$ nanoparticles, it is important for the magnetization easy axis to be oriented, since the switching field has an angular dependence, i.e., by diverging from the perpendicular direction the coercivity will be decreased.[8] It is well known that the structure of the substrate material mainly determines the film orientation. For example, in the case of sequentially evaporated Pd and Fe layers, the Pd layer grows epitaxially on the surface of MgO(001) or NaCl(001) single-crystalline substrates,[9] and after the annealing process, the $L1_0$ phase with a ⟨001⟩ orientation is formed in both cases. In the case of nanoparticle structures, any one of the three ⟨100⟩ axes of the fcc Pd or Pt parent structure can correspond to the tetragonal *c* axis, i.e., *not all* of the annealed $L1_0$ particles have their *c* axis perpendicular to the film plane.[10]

In this work, we propose an effective procedure to reduce the $L1_0$ ordering temperature and to prepare individual nanoparticle structures with a preferential *c*-axis orientation by the addition of Co to Fe–Pd nanoparticles. Co has a similar atom size as Fe; therefore it is expected to replace Fe in the $L1_0$ structure. Also, the addition of Co to Fe leads to a high magnetization of the material according to the Slater-Pauling curve.[11] This means that the magnetic moment of the $L1_0$-PdCoFe nanoparticles is expected to increase with Co additions, besides the improvements of perpendicular magnetization and a low formation temperature for the $L1_0$ phase. PdCoFe nanocrystalline samples with different Co concentrations were prepared for structural and magnetic property analysis, as described in the following section.

II. EXPERIMENTAL PROCEDURE

Magnetic nanocrystals were prepared by sequential evaporation of Pd, Co, and Fe onto NaCl(001) single-crystalline substrates in a high-vacuum chamber with a base pressure of 1×10^{-6} Pa. The substrate temperature during evaporation was 473 K. A quartz crystal monitor was used to measure the deposition rate and thickness of the layers. A 10-nm-thick amorphous Al_2O_3 layer was deposited onto the nanoparticles to protect the sample from oxidation and to make the nanoparticles self-supporting. Samples with different compositions were fabricated by changing the deposited thickness of the materials. The Co content was varied from 5 to 18 at. % by decreasing the Fe content without changing the Pd content. The Al_2O_3 layers with the nanoparticles were wet stripped from the substrate and mounted on Cu grids. Morphological and structural analyses of the samples were performed by transmission electron microscope (TEM) (JEOL JEM-3000F). The chemical composition of the nano-

[a]Electronic mail: andras22@sanken.osaka-u.ac.jp

TABLE I. Alloy compositions of the Pd–Co–Fe nanoparticle determined by EDS and mean-particle sizes (d) with standard deviation ($\ln \sigma$) of the samples with different Co concentrations.

	Composition		Mean-particle size	
Sample	Pd/(Co+Fe) (at. %)	Co (at. %)	d (nm)	$\ln \sigma$
A	55/45	5	8.23	0.27
B	53/47	9	8.06	0.26
C	51/49	12	8.85	0.19
D	51/49	18	9.09	0.24

particles was determined using an energy-dispersive x-ray spectrometer (EDS) attached to the TEM. To follow the $L1_0$ phase formation process, *in situ* annealing of selected samples was performed in the TEM between 573 and 873 K. During the annealing process, the temperature was measured by Pt–PtRh thermocouple attached to the sample holder close to the specimen. In view of the results of the *in situ* experiments, postdeposition annealing was performed at 798 K for 1 h in a high-vacuum furnace ($<2\times10^{-5}$ Pa) to obtain a highly ordered $L1_0$ structure of Pd–Co–Fe. Magnetic properties were measured using a superconducting quantum interference device (SQUID) magnetometer (Quantum Design, MPMS-XL) at 300 and 10 K with a magnetic field up to 30 kOe. The magnetic field was applied both parallel and perpendicular to the sample plane.

III. RESULTS AND DISCUSSION

A. Structure and morphology of as-deposited Pd–Co–Fe films

The composition, Co concentration, and mean-particle size of the as-prepared series of samples, labeled A–D, are listed in Table I. Since no remarkable difference in the structure and morphology of the samples was found, only sample B will be analyzed in detail in the following. Figure 1(a) shows a bright-field (BF) TEM image of the as-prepared nanocrystalline structure, which consists of individual particles. The growth mode of the particles corresponds to the Volmer-Weber type, in which separated three-dimensional (3D) crystals grow. Some particles are also coalesced. The corresponding selected-area electron diffraction (SAED) pattern shows a [001] zone-axis diffraction pattern of the fcc structure [Fig. 1(b)]. The weak halo pattern of the supporting amorphous Al_2O_3 layer can also be observed in the SAED pattern. Detailed analysis of the diffraction pattern reveals that two phases formed simultaneously in the nanoparticles. The strong reflections are related to fcc Pd, while the additional weak reflections are related to bcc CoFe phase. This composite phase formation was verified by comparing the SAED pattern with a simulated SAED pattern (not shown here) using the x-ray powder diffraction database for the crystallographic data.[14] From the electron diffraction analysis, the epitaxial growth of the CoFe on seed Pd nanoparticles could be determined with a mutual orientation relationship: $[001]_{Pd}\|[001]_{FeCo}$, $(100)_{Pd}\|(110)_{FeCo}$. Figure 1(c) shows a high resolution TEM (HRTEM) image of the as-prepared Pd/CoFe nanoparticles. The dark contrast visible along the particle can be attributed to the strain field that originates from the lattice mismatch between the Pd and CoFe phases; however, the other possibilities causing the contrast (geometry and thickness of the particles) cannot be excluded unambiguously. The particle size distribution was defined by measuring the diameters in BF images and fitting with a log-normal distribution function (Table I).

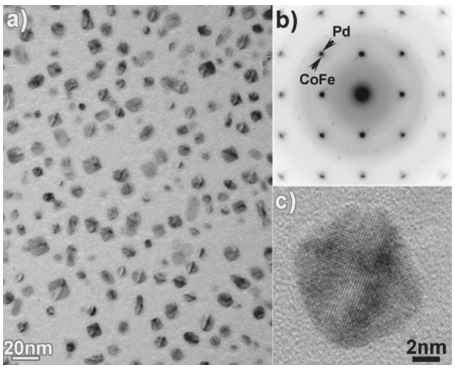

FIG. 1. BF-TEM image (a) and corresponding SAED pattern (b) of as-prepared Pd/CoFe particles. In the SAED pattern Pd and CoFe reflections can be separated. A high resolution TEM image (c) of Pd/CoFe particle.

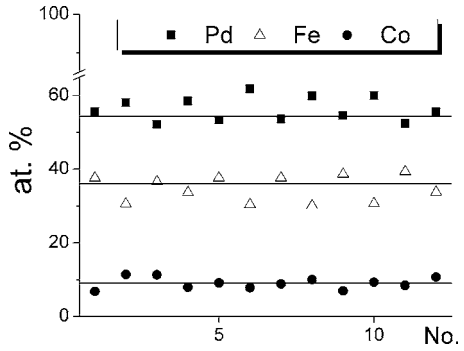

FIG. 2. The composition analysis of individual Pd/CoFe particles by nanobeam EDS. The number of measurements are indicated in the horizontal axis. The horizontal lines indicate the results of large area EDS analysis.

The chemical composition of the nanoparticles was obtained by EDS. First, the average sample composition was determined using a selected area of 50 μm in diameter and including several thousands of nanoparticles. Then, a nanoprobe electron beam with a diameter of about 4 nm (full width at half maximum) was formed, making it possible to identify the composition of individual nanoparticles. The results obtained on sample B with 9 at. % Co are summarized in Fig. 2. The compositions of the selected Pd/CoFe nanoparticles were nearly the same as that of the average sample composition.

B. $L1_0$ ordered phase formation by heat treatment

In situ TEM annealing of the Pd/CoFe nanoparticles was performed in order to analyze the $L1_0$ phase formation. Morphological and structural changes that occurred during the annealing process were followed by recording BF TEM images and SAED patterns. No structural change was observed in the SAED pattern at 673 K [Fig. 3(a)]. Weak 110 superlattice reflections of the $L1_0$ ordered structure appeared at

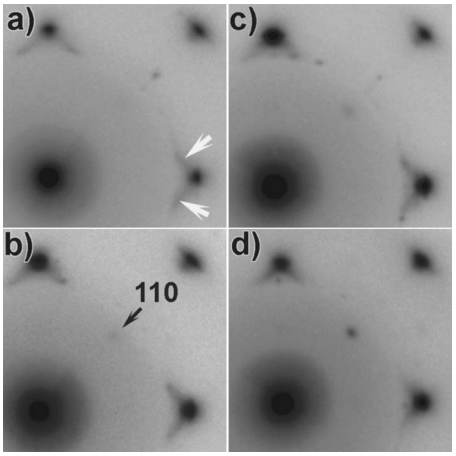

FIG. 3. A series of SAED patterns taken at 673 K (a), 698 K (b), 723 K (c), and 773 K (d) during the *in situ* TEM annealing. The weak 110 superlattice reflection starts to appear at 698 K (b), indicating the atomic ordering. Besides the fundamental reflections, there exist extra reflections [as marked by arrows in (a)] from {111} twins and stacking faults.

698 K [Fig. 3(b)]. The intensity of the superlattice reflections became stronger with increasing temperature as ordering proceeded [Figs. 3(c) and 3(d)]. The present results indicate that adding Co to the Pd–Fe nanoparticles effectively reduces the ordering temperature by 50 K, as compared to binary Pd–Fe nanoparticles with a similar structure.[10] Besides the appearance of the 110 superlattice reflections, additional reflections due to {111} twins and stacking faults[12] are clearly visible in the SAED patterns, as shown by arrows in Fig. 3(a), and this intensity decreases at 773 K.

The local structure of the postdeposition annealed nanoparticles was analyzed by HRTEM images and nanobeam electron diffraction. Figure 4(a) shows a HRTEM image of $L1_0$-PdCoFe nanoparticle. The large lattice spacing (~0.27 nm) of the (110) planes is clearly visible. The particle shape can be recognized as octahedral, truncated at the edges and with extended {001} planes. The nanobeam diffraction pattern in Fig. 4(b) shows that the particle is composed of a single variant with the *c* axis oriented perpendicular to the film plane. It is noteworthy that 001 superlattice reflections are not visible in the SAED pattern [Fig. 4(c)], indicating that a large number of particles form with preferential orientation of the crystallographic *c* axis perpendicular to the film plane. In order to determine the amount of nanoparticles with this preferential orientation, a combined analysis of SAED patterns and dark-field (DF) TEM images were performed, where the DF images were taken with 110 and 200 reflections of the $L1_0$ phase. The results indicated that more than 80% of the nanoparticles have their *c* axis perpendicular to the film plane, according to the areal number density of the bright nanoparticle contrast. Consistent results were obtained on other samples analyzed in the same way. It should be noted that approximately 50% of $L1_0$-PdFe nanoparticles[10] have a *c*-axis orientation perpendicular to the film plane, while Pd–Fe nanoparticles with Cu additives have 74%.[7] These experimental results indicate that adding Co to the Fe–Pd nanoparticles enhances the *c*-axis orientation of the $L1_0$ structure perpendicular to the film plane. In order to analyze the importance of the evaporation sequence, Co was

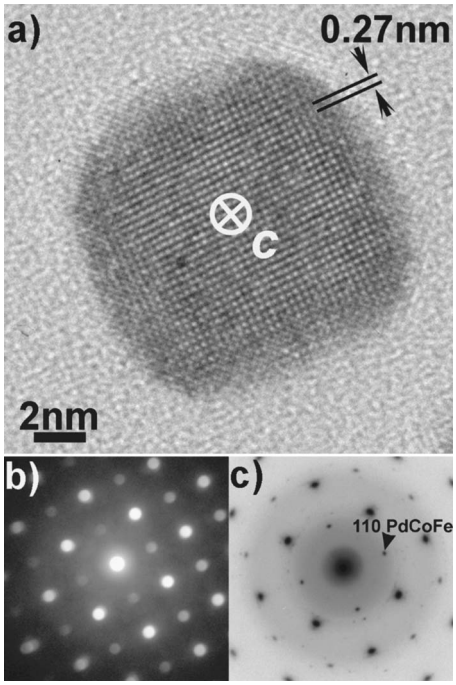

FIG. 4. A high resolution TEM image of the $L1_0$-PdCoFe nanoparticle (from sample B) with *c* axis perpendicular to the film plane (a). Nanobeam electron diffraction (b) from one particle and SAED pattern from large area (c).

deposited on top of existing Fe–Pd nanoparticles. However, the structure and magnetic properties of this sample revealed no remarkable differences in the *c*-axis orientation and magnetic coercivity with respect to the location of Co. Thus the role of Co in the development of the preferential *c*-axis orientation is not well understood at present and further studies are necessary to clarify it.

The lattice parameters of the $L1_0$-PdCoFe phase were calculated using Vegard's law for a ternary composition by replacing Fe atoms with Co. It is well known that the $L1_0$ tetragonal structure represents a stacking sequence of the atomic planes of the components along the *c* axis. The replacement of Fe atoms with smaller atoms such as Co [r_{Fe} =0.156 nm, r_{Co}=0.152 nm (Ref. 13)] causes a decrease in the lattice parameter *c*. In our experiments, the Co concentration was varied between 5 and 18 at. % (Table I), so that the *c* axis should decrease from 0.3657 to 0.3651 nm according to Vegard's law, while the *a* axis should remain almost unchanged (a=0.381 nm).

C. Magnetic properties of the $L1_0$-PdCoFe nanoparticles

Figure 5(a) shows the magnetic hysteresis loops measured on sample A, which displayed the highest perpendicular coercivity in the samples. In all samples, the magnetization curves measured along the film normal showed considerably higher coercivities compared to the in-plane ones. This feature corresponds to the strong preferred perpendicular orientation of the magnetic easy axis (*c* axis) of the particles, which was previously demonstrated by the SAED DF analyses. Sample A with 5 at. % Co had the maximum perpendicular coercivity of 1.75 kOe at room tempera-

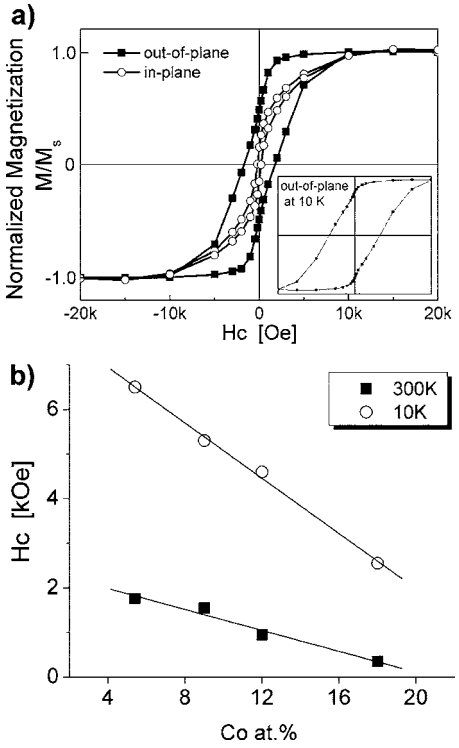

FIG. 5. Magnetic hysteresis loops (a) of the annealed sample A measured at 300 K with external magnetic field along the perpendicular and in-plane directions to the film plane. Inset: loop measured at 10 K in the perpendicular direction. The magnetic coercivity (b) changes of the samples with different Co concentrations measured in perpendicular direction at 300 K (solid rectangles) and 10 K of annealed samples (open circles).

ture, while the in-plane value was 0.19 kOe. In this sample, the perpendicular coercivity increased up to 6.5 kOe at 10 K due to a decrease in the thermal agitation of the magnetic moment and to an increase of the magnetocrystalline anisotropy constant. For the magnetization curves of samples A and B measured at room temperature along the perpendicular direction, the ratio of the remanence magnetization (M_r) to the saturation magnetization (M_s) was equal to 0.5. The M_r/M_s value decreased to 0.2 with an increase in the Co concentration to 18 at. %. Here, shearing corrections were not performed, since an accurate demagnetizing factor and the aspect ratio of the nanoparticles were not known. The magnetic coercivity of the nanoparticles gradually decreased with increasing Co concentration [Fig. 5(b)]. Even though Co additions slightly decrease the coercivity of $L1_0$ nanoparticles compared to pure Pd–Fe, it still can be adequate for perpendicular magnetic recording media applications. Moreover, from these results, we can suggest that $L1_0$-$Pd_{52}(CoFe)_{48}$ nanoparticles with Co concentrations less than 10 at. % offer a good performance for probable magnetic applications.

IV. CONCLUSIONS

In this work, the effects of Co additions on the atomic ordering and hard magnetic properties of $L1_0$-PdFe films were examined as a function of the Co concentration. Nanoparticles with a fixed mutual orientation between the fcc Pd and bcc CoFe phases were formed by sequential deposition of the components. *In situ* TEM annealing revealed that the $L1_0$ phase starts to form at 698 K, i.e., that the addition of Co to binary Pd–Fe nanoparticles can effectively reduce the formation temperature of the ordered phase by 50 K. The $L1_0$-PdCoFe nanoparticles show excellent perpendicular anisotropy due to the preferential magnetic easy axis orientation perpendicular to the film plane. A maximum perpendicular coercivity of 1.75 kOe was measured at room temperature for nanoparticles of 8 nm in diameter.

ACKNOWLEDGMENTS

One of the authors (A.K.) greatly acknowledges the financial support and fellowship from the Japan Society for the Promotion of Science. This study was partly supported by the Grant-in-Aid for Scientific Research (S) (No. 16106008) from the Ministry of Education, Culture, Sports, Science and Technology, Japan.

[1]H. Shima, K. Oikawa, A. Fujita, K. Fukamichi, K. Ishida, and A. Sakuma, Phys. Rev. B **70**, 224408 (2004).
[2]S. Sun, C. B. Murray, D. Weller, L. Folks, and A. Moser, Science **287**, 1989 (2000).
[3]M. Weisheit, L. Schultz, and S. Fahler, J. Appl. Phys. **95**, 7489 (2004).
[4]B. Bian, K. Sato, Y. Hirotsu, and A. Makino, Appl. Phys. Lett. **75**, 3686 (1999).
[5]T. Maeda, T. Kai, A. Kikitsu, T. Nagase, and J. Akiyama, Appl. Phys. Lett. **80**, 2147 (2002).
[6]Y.-N. Hsu, S. Jeong, D. E. Laughlin, and D. N. Lamberth, J. Appl. Phys. **89**, 7068 (2001).
[7]H. Naganuma, K. Sato, and Y. Hirotsu, J. Appl. Phys. **99**, 08N706 (2006).
[8]S. Okamoto, O. Kitakami, N. Kikuchi, T. Miyazaki, and Y. Shimada, Phys. Rev. B **67**, 094422 (2003).
[9]A. Kovács, K. Sato, and Y. Hirotsu, Proceedings of the 16th International Microscopy Congress, 2006, p. 1520.
[10]K. Sato and Y. Hirotsu, J. Appl. Phys. **93**, 6291 (2003).
[11]R. C. O'Handley, *Modern Magnetic Materials: Principles and Applications* (Wiley, New York, 2000), p. 145.
[12]B. Bian, D. E. Laughlin, K. Sato, and Y. Hirotsu, J. Appl. Phys. **87**, 6962 (2000).
[13]Atomic radius data of Fe and Co from www.webelements. com
[14]JCPDS Card No. 05-0681; JCPDS Card No. 49-1568.